

# Four-wing hyperchaotic attractor generated from a new 4D system with one equilibrium and its fractional-order form

Sara Dadras · Hamid Reza Momeni ·  
Guoyuan Qi · Zhong-lin Wang

Received: 31 October 2010 / Accepted: 19 April 2011 / Published online: 12 May 2011  
© Springer Science+Business Media B.V. 2011

**Abstract** In this paper, a new simple 4D smooth autonomous system is proposed, which illustrates two interesting rare phenomena: first, this system can generate a four-wing hyperchaotic and a four-wing chaotic attractor and second, this generation occurs under condition that the system has only one equilibrium point at the origin. The dynamic analysis approach in the paper involves time series, phase portraits, Lyapunov exponents, bifurcation diagram, and Poincaré maps, to investigate some basic dynamical behaviors of the proposed 4D system. The physical existence of the four-wing hyperchaotic attractor is verified by an electronic circuit. Finally, it is shown that the fractional-order

form of the system can also generate a chaotic four-wing attractor.

**Keywords** Four-wing hyperchaotic attractor · Lyapunov exponent · Poincaré mapping · Fractional-order system

## 1 Introduction

Near half a century has passed since the first chaotic system was reported by Lorenz [1]. In two last decades, study of chaotic systems has gained many interests and has found applications in different areas ranging from engineering to ecology [2–5]. But, still there is no unified theory of chaos from which the existence of chaotic behaviors can be predicted, and generally, the new chaotic systems are introduced in the form of mathematical models and verified via numerical simulations.

For years, almost all the reported chaotic systems are the systems with two-wing chaotic attractors [6–10]. But, in the last decade, research for more complex chaotic systems has led to the finding of the multi-wing chaotic systems. The multi-wing chaotic systems can be classified into two totally different groups. The first class or the Lorenz-like chaotic systems [11–13] are the systems with smooth nonlinearities in which the number of wings is not equal to that of the equilibria. The second class or the Chua-like chaotic systems

---

S. Dadras · H.R. Momeni (✉)  
Automation and Instruments Lab, Electrical Engineering  
Department, Tarbiat Modares University, P.O. Box  
14115-143, Tehran, Iran  
e-mail: [momeni\\_h@modares.ac.ir](mailto:momeni_h@modares.ac.ir)

S. Dadras  
e-mail: [s\\_dadras@modares.ac.ir](mailto:s_dadras@modares.ac.ir)

S. Dadras  
e-mail: [s\\_dadras@yahoo.com](mailto:s_dadras@yahoo.com)

G. Qi  
Department of Electrical Engineering, Tshwane University  
of Technology, Pretoria 0001, South Africa

Z.-l. Wang  
Department of Physics and Electronics, Binzhou  
University, Binzhou 256603, Shandong, China

[14–16] are the systems that have non-smooth nonlinear parts. In these systems, the basic technique to generate different number of scrolls is increasing the number of equilibrium points and the number of scrolls equals to that of the equilibria. Although it is more difficult to obtain a chaotic attractor with more than double wings from a smooth dynamical system, some four-wing Lorenz-like chaotic systems have been introduced in recent years [12, 13, 17–22]. All these systems have five equilibrium points and each wing wonders around a nonzero equilibria.

In 1979, Rössler reported a novel complex dynamical system with a new criterion [23]. Unlike the other known chaotic systems up to that time, his system has two positive Lyapunov exponents. Having more than one positive Lyapunov exponents causes the system to show behavior with a high degree of disorder and randomness. Nowadays, these systems are called hyperchaotic systems. In recent years, notable contribution has been made to generation of hyperchaotic systems with more complex dynamics, and this new concept has become a very important research topic.

Nearly all the 4D hyperchaotic systems, reported up to now, have double-wing hyperchaotic attractors with three or five equilibrium points [24–39]. Generating a hyperchaotic attractor from a smooth dynamical system with one equilibrium point is a very rare phenomenon [31, 40, 41]. The attractors evolved from these systems are butterfly-shaped with two wings. Another very rare phenomenon about the hyperchaotic systems is that they can generate four-wing attractor [42]. The Cang's system is hyperchaotic and four-winged, but it has five equilibrium points. Normally, a four-wing hyperchaotic attractor can be generated from a nonlinear system of more than four differential equations [43]. So far, in literature, there is no reported 3D or 4D smooth autonomous system with only one equilibrium that can generate a four-wing and hyperchaotic attractor.

Fractional calculus is more than three centuries old topic, and recently the applications of fractional calculus have been overgrowing [44–47]. The study of the dynamic systems of fractional order has attracted increasing interest from many researchers. It has been demonstrated that some fractional-order differential systems behave chaotically or hyperchaotically, such as the fractional-order Chen system [48], the fractional-order Chua system [49], the fractional-order Liu system [50], the fractional-order coupled

Lorenz system [51], and the fractional-order Rössler system [52].

In this paper, we introduce a new four-dimensional smooth autonomous hyperchaotic system. This system has two important dynamics: first, it can generate a four-wing hyperchaotic attractor and a four-wing chaotic attractor and second, it has only one equilibrium point which is located at the center of the whole attractor. Besides, the fractional-order version of this new system shows chaotic behavior and can generate chaotic four-wing attractors. The paper is organized as follows: In Sect. 2, the new system is briefly introduced. In Sect. 3, varying one system parameter, different dynamical behaviors of the system are discussed. Three different methods for analyzing chaotic systems, Lyapunov exponent diagram, bifurcation diagram and Poincaré mapping, are interpreted in Sects. 4 and 5. In Sect. 6, a physical FPGA circuit is built to confirm the numerically simulated four-wing hyperchaotic attractor. Explanation about the existing methods of approximated solution of fractional differential equations and simulation results of the fractional-order form of the new chaotic system are included in Sects. 7 and 8, respectively. Finally, some concluding remarks are given in Sect. 9.

## 2 The proposed 4D dynamical system

Consider the following simple 4D quadratic smooth autonomous system:

$$\begin{cases} \dot{x} = ax - yz + w, \\ \dot{y} = xz - by, \\ \dot{z} = xy - cz + xw, \\ \dot{w} = -y, \end{cases} \quad (1)$$

where  $[x, y, z, w]^T \in R^4$  is the state vector, and  $a, b$  and  $c$  are positive constant parameters of the system. In the following, some basic properties of system (1) are analyzed.

### 2.1 Dissipativity and existence of attractor

To ensure that system (1) is chaotic, the general condition of dissipativity should be considered, i.e.

$$\nabla V = \frac{\partial \dot{x}}{\partial x} + \frac{\partial \dot{y}}{\partial y} + \frac{\partial \dot{z}}{\partial z} = a - b - c < 0. \quad (2)$$

Thus, for  $a < b + c$ , system (1) is dissipative. It means that a volume element  $V_0$  is contracted by the flow into a volume element  $V_0 e^{\nabla V t}$  in time  $t$ . That is, each volume containing the system orbit shrinks to zero as  $t \rightarrow \infty$  at an exponential rate  $\nabla V$ , which is independent of system states. Consequently, all system orbits will ultimately be confined to a specific subset of zero volume and the asymptotic motion settles onto an attractor. Then, the existence of an attractor is proved.

### 2.2 Symmetry and invariance

The new chaotic system (1) is invariant under the coordinate transform  $(x, y, z, w) \rightarrow (-x, -y, z, -w)$ , i.e. the system (1) is symmetrical about the coordinate axis  $z$ .

### 2.3 Equilibria and stability

The equilibria of system (1) can be found by solving the following algebraic equations simultaneously:

$$\begin{cases} ax - yz + w = 0, \\ xz - by = 0, \\ xy - cz + xw = 0, \\ -y = 0. \end{cases} \tag{3}$$

From the fourth equation of (3), one has

$$y = 0. \tag{4}$$

Substituting this into the other three equations of (3) yields

$$\begin{cases} ax + w = 0, \\ xz = 0, \\ -cz + xw = 0. \end{cases} \tag{5}$$

So, it can be concluded that

$$x = \frac{-1}{a}w \quad \text{and} \quad z = \frac{1}{c}xw = \frac{-1}{ca}w^2. \tag{6}$$

Furthermore, from (6) and the second equation of (5), it can be deduced that

$$w = 0. \tag{7}$$

Hence,  $O(0, 0, 0, 0)$  is the only equilibrium point of the system (1).

Here, the stability of the zero equilibrium  $O$  is discussed. By linearizing the system (1) at  $O$ , one obtains

the Jacobian

$$J = \begin{bmatrix} a & -z & -y & 1 \\ z & -b & x & 0 \\ y + w & x & -c & x \\ 0 & -1 & 0 & 0 \end{bmatrix}$$

$$\xrightarrow{O(0,0,0,0)} J_O = \begin{bmatrix} a & 0 & 0 & 1 \\ 0 & -b & 0 & 0 \\ 0 & 0 & -c & 0 \\ 0 & -1 & 0 & 0 \end{bmatrix}. \tag{8}$$

So, the eigenvalues of the linearized system are obtained as follows:

$$\begin{aligned} |\lambda I - J_O| = 0 &\Rightarrow \lambda_1 = 0, \quad \lambda_2 = a, \\ \lambda_3 = -b, \quad \lambda_4 = -c. \end{aligned} \tag{9}$$

Since  $a, b$ , and  $c$  are all positive real numbers, one can easily find  $\lambda_3, \lambda_4 < 0, \lambda_2 > 0$ , implying that the equilibrium  $O$  is unstable, i.e. origin is an unstable saddle point for system (1).

## 3 Dynamical behavior of the new system

System (1) has been found to be hyperchaotic and chaotic over a wide range of parameters. Remarkably, this system can display four-wing hyperchaotic and four-wing chaotic attractors while the system has only one equilibrium point, which is unusual for a four-dimensional smooth nonlinear system.

*Remark 1* It is notable that all the 4D smooth systems generating four-wing attractors, which were reported up to now, have at least five equilibria. In these systems, the nonzero equilibrium points are located at the centers of each wing of the attractor, and the origin is the center of the whole four-wing chaotic attractor.

### 3.1 Four-wing hyperchaotic attractor

In this section, the numerical simulations are carried out using MATLAB program. The fourth order Runge–Kutta integration algorithm was performed to solve the differential equations. The initial condition is set to  $[10, 1, 10, 1]^T$ .

The new system can display a four-wing hyperchaotic attractor if the parameters are properly chosen. Setting the parameters  $a = 8, b = 40$  and  $c = 14.9$ , as is seen in Fig. 1, the system has generated a four-wing

**Fig. 1** Phase portraits of the four-wing hyperchaotic attractor for  $a = 8, b = 40, c = 14.9$

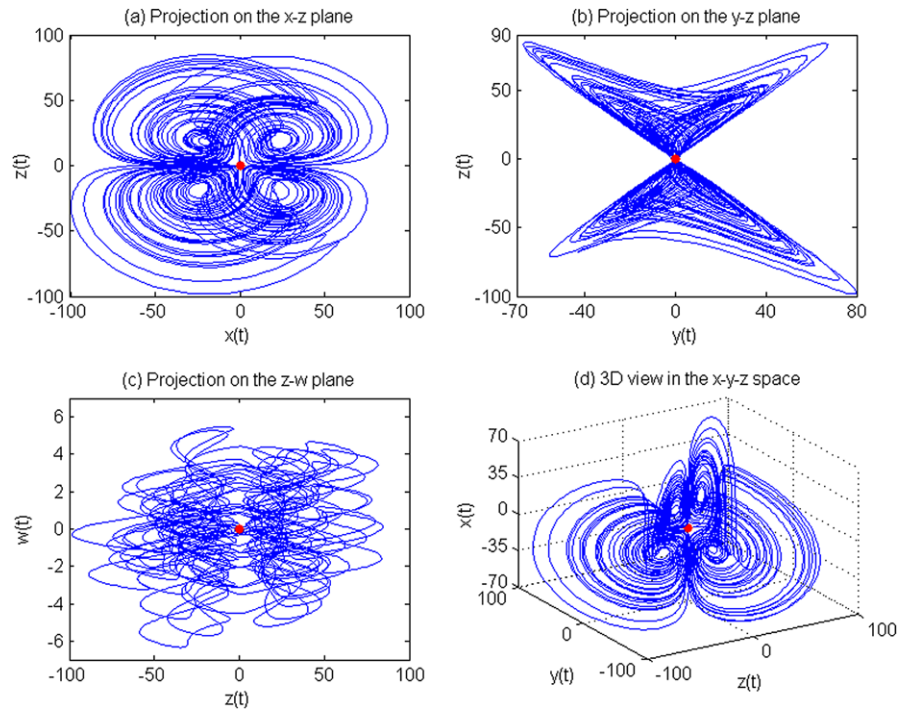
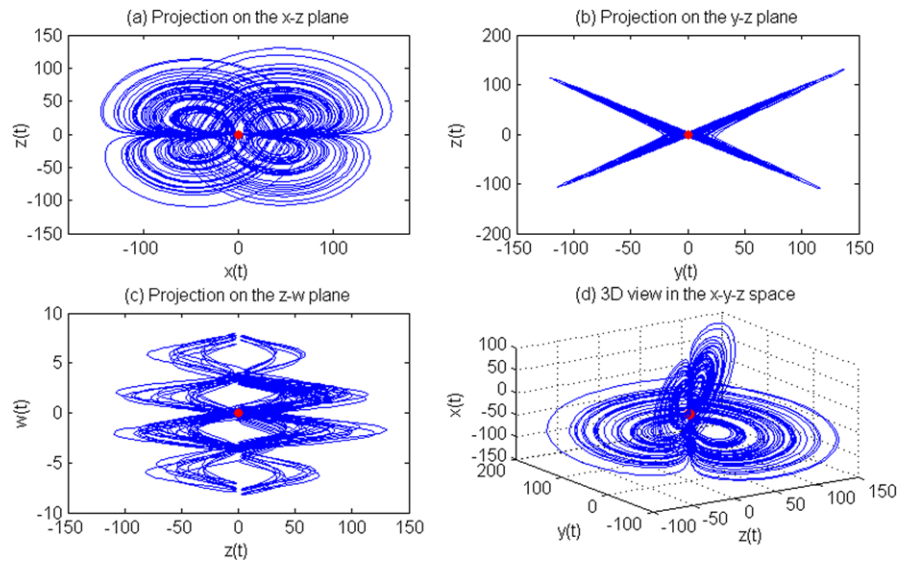


**Fig. 2** Phase portraits of the four-wing chaotic attractor for  $a = 8, b = 40, c = 49$

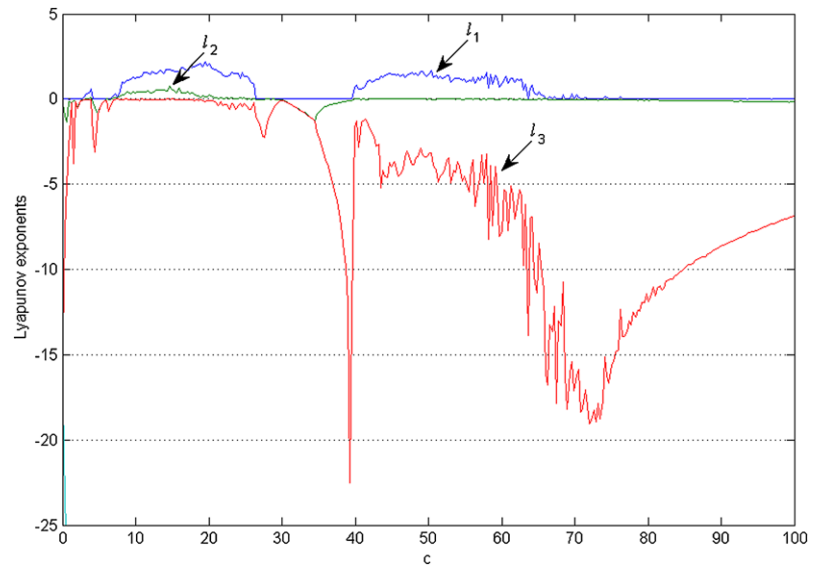


hyperchaotic attractor. System (1) has only one equilibrium which is depicted as a red dot in Fig. 1. It is notable that there exist many orbits freely running in the 3D space and system trajectories can cross the boundary lines to the other side. It can be clearly seen that the origin is the center of the whole hyperchaotic attractor.

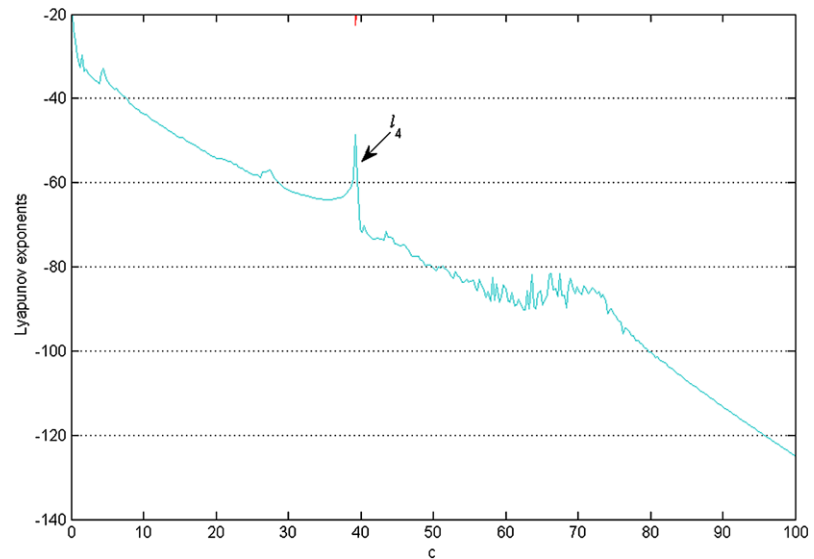
It is clearly observed that the four sub-attractors look like the inner corners of four connected eddies.

Each two pairs of wings connected resemble the butterfly shape of the Lorenz chaotic attractor, which as a whole forms a singular tornado-like shape with four inner holes. It seems the four inner holes would be the four equilibria beside the origin. However, they do not exist at all, which is proved via (3)–(7). Moreover, the Lyapunov exponents have been calculated as  $l_1 = 1.844016, l_2 = 0.500061, l_3 = 0, l_4 = -49.212797,$

**Fig. 3** Lyapunov exponents' spectrum of the system (1) versus parameter  $c$



(a)



(b)

indicating the system is hyperchaotic with the aforementioned set of parameters.

### 3.2 Four-wing chaotic attractor

Setting the parameters as  $a = 8, b = 40$  and  $c = 49$ , the system (1) is chaotic and can generate a four-wing chaotic attractor which is shown in Fig. 2. The Lyapunov exponents of the system in this case are  $l_1 = 1.508572, l_2 = 0, l_3 = -3.327860, l_4 = -79.153856$ . It ought to be stressed that the effect of initial condi-

tions on the four-wing chaotic attractor is not visible, i.e. the system can generate a four-wing chaotic attractor with any desired initial condition and the four-wing chaotic attractor is independent of initial values.

### 4 Lyapunov spectra and bifurcation diagram

When the parameters  $a = 8$  and  $b = 40$  are fixed while parameter  $c$  is varied, the spectrum of Lyapunov exponents and the corresponding bifurcation diagram of

state  $z$  with respect to  $c$  are obtained as shown in Figs. 3 and 4, respectively.

When  $c < 2.5$ , the maximum Lyapunov exponent equals zero, implying that the new system (1) exhibits periodic behavior; while for  $c \in [2.5, 3.2]$ , the maximum Lyapunov exponent is positive, implying

that the system is chaotic. In the region  $3.2 < c < 4$ , the system is hyperchaotic with two positive Lyapunov exponents. Again, when  $4 \leq c \leq 6$ , the maximum Lyapunov exponent is zero. The system displays quasi-periodic motion for  $6 < c < 6.6$ . In the region  $c \in [6.6, 22]$ , the system (1) is hyperchaotic. The system shows chaotic behavior for  $22 < c < 26.4$ . For  $26.4 \leq c < 29.9$ , the system has two zero Lyapunov exponents implying that the system is quasi-periodic. In the region  $29.9 < c < 39.6$ , the new system exhibits a periodic behavior. The system is chaotic in the area  $39.6 \leq c < 66$ . For  $66 \leq c < 81.2$ , the system displays a quasi-periodic motion. In the aforementioned interval, there are some tiny periodic and chaotic subregions. Finally, when  $c \geq 81.2$ , the maximum Lyapunov exponent almost equals zero and the system eventually evolves into a periodic orbit. The whole evolution process can be clearly seen from the bifurcation diagram shown in Fig. 4, which illustrates the dynamics of state variables. Figure 5, in which the initial transients have been omitted for clarity, shows two different periodic behaviors of the system (1) for  $c = 69.4$  and  $c = 35$ , respectively. The quasi-periodic behavior of the system for  $c = 28$  can be seen in Fig. 6.

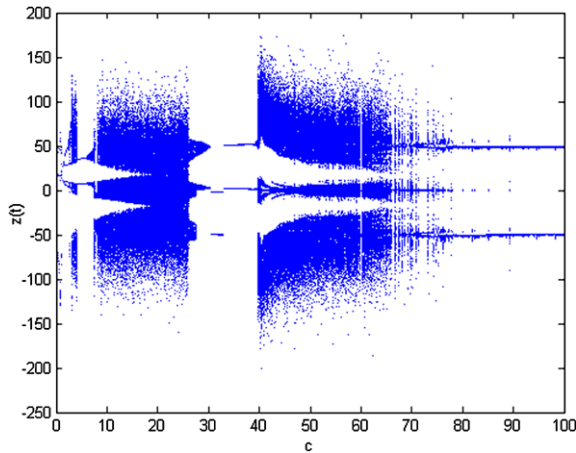


**Fig. 4** Bifurcation diagram of the system (1) third state versus parameter  $c$

**Fig. 5** Phase portraits of the periodic orbits for  $a = 8, b = 40$ , (a, b)  $c = 69.4$ , (c, d)  $c = 35$

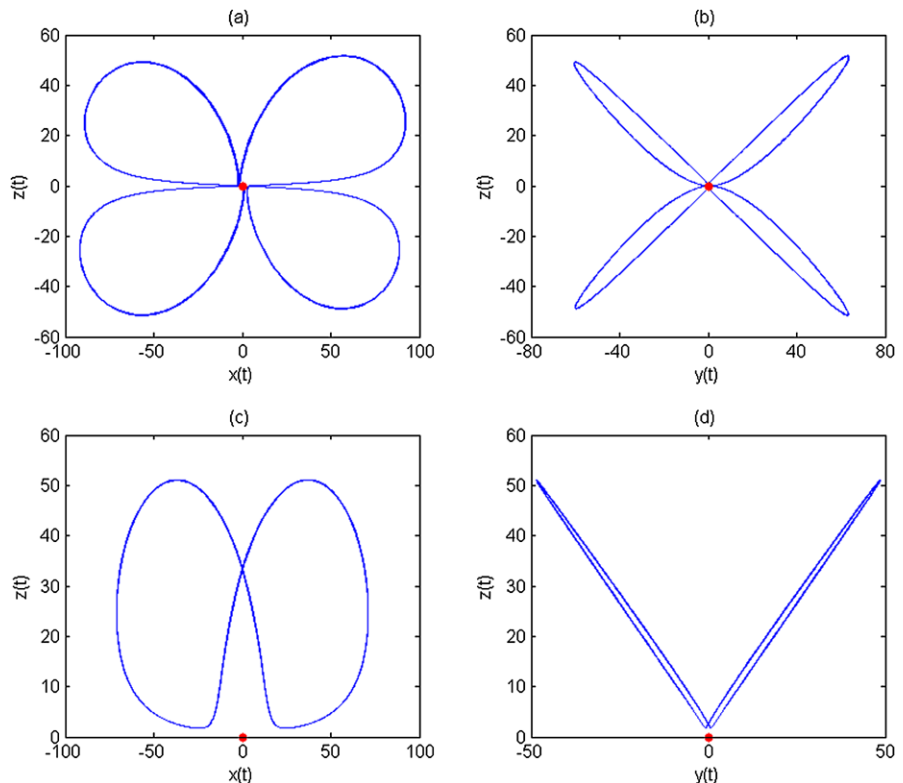
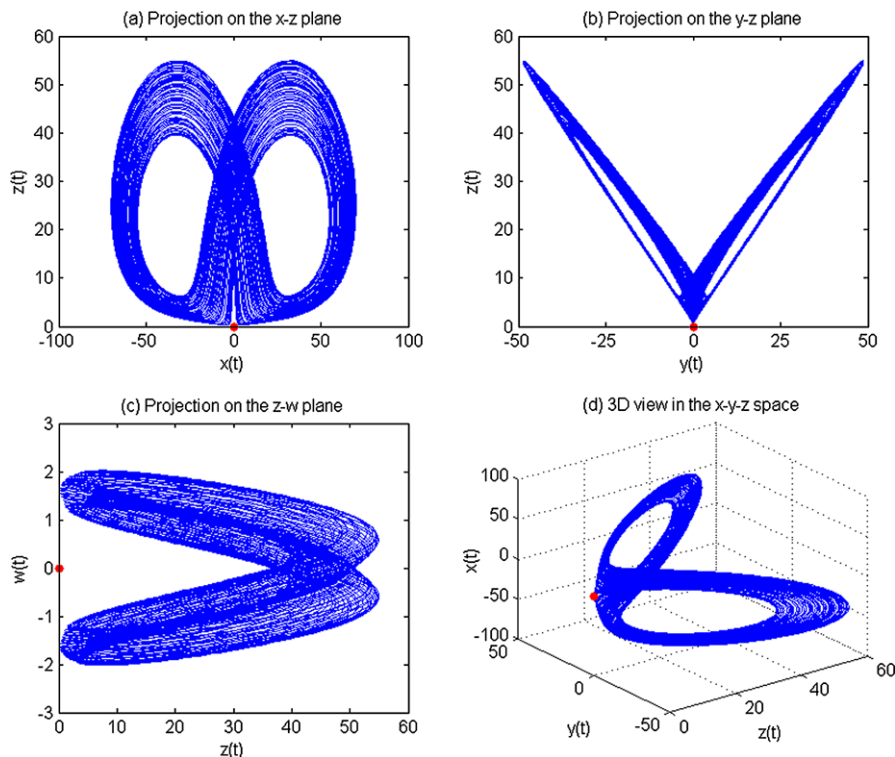


**Fig. 6** Phase portraits of the quasi-periodic orbits for  $a = 8, b = 40, c = 28$



**5 Poincaré mapping**

As an important analysis technique, the Poincaré map can reflect bifurcation and folding properties of chaos. We have taken

$$\begin{aligned}
 \Sigma_1 &= \{[x, y, z, w]^T \in R^4 \mid x = 0\} \\
 \Sigma_2 &= \{[x, y, z, w]^T \in R^4 \mid y = 0\} \\
 \Sigma_3 &= \{[x, y, z, w]^T \in R^4 \mid w = 0\} \\
 \Sigma_4 &= \{[x, y, z, w]^T \in R^4 \mid w - 2y = -1\}
 \end{aligned}
 \tag{10}$$

as cross sections and the system parameters are set to  $a = 8, b = 40$  and  $c = 14.9$ . Figure 7(a)–(d), shows projections of the Poincaré map on  $y - z, z - x$  and  $x - z$  planes. From the figure one can see that the Poincaré map here consists of several limbs with various bifurcations in different directions, which indicates that the system has extremely rich dynamics. Also, the Poincaré maps show that the branches are jointed and united as a single attractor. This proves the existence of the four-wing hyperchaotic attractor in Fig. 1.

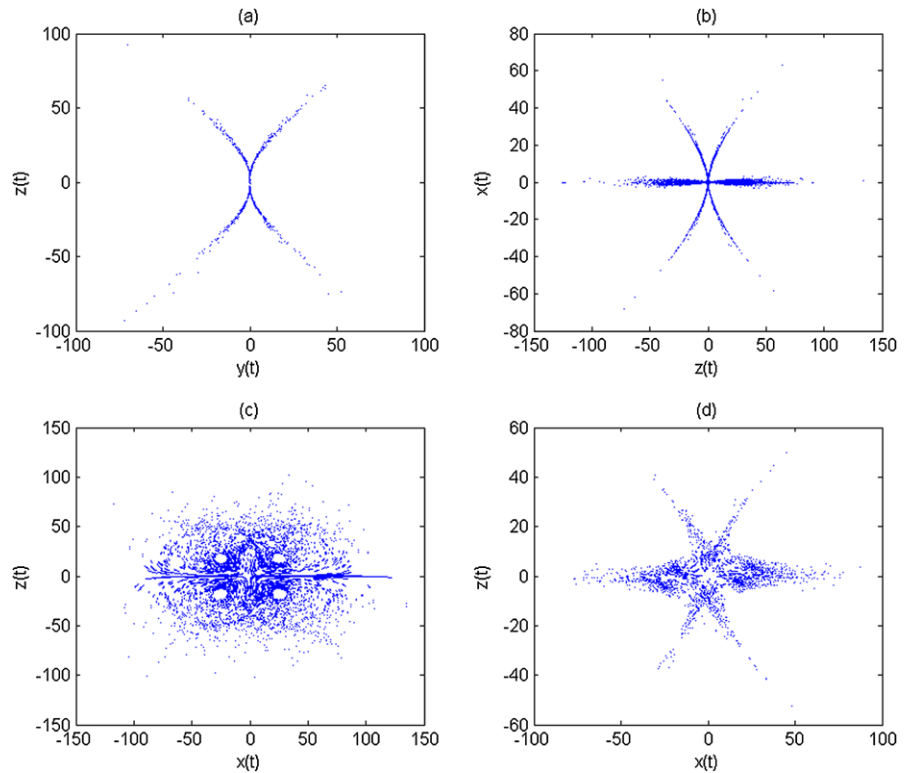
**6 Verification via circuit experiment**

An FPGA electronic circuit is designed to realize the 4D hyperchaotic system (1) with parameters  $a = 8, b = 40$  and  $c = 14.9$ . The experimental observations from the analog oscilloscope are shown in Fig. 8(a)–(f). It can be clearly seen that this experiment shows that the system with the above-mentioned parameters can generate a real four-wing hyperchaotic attractor. Comparing the numerical simulation and the circuit experimental results it can be declared that a very good qualitative agreement between the two parts has been confirmed.

**7 Numerical algorithm for simulation of fractional-order systems**

The numerical calculation of a fractional differential equation (FDE) is not as simple as that of an ordinary differential equation. Two approximation methods have been developed for numerical solution of a fractional differential equation in the literature. These methods can be applied to both linear and nonlinear fractional-order systems. One is the time-domain

**Fig. 7** Poincaré maps of the four-wing hyperchaotic attractor with parameters  $a = 8, b = 40, c = 14.9$ , on different crossing sections: **(a)**  $x = 0$ , **(b)**  $y = 0$ , **(c)**  $w = 0$ , **(d)**  $w - 2y = -1$



method which is a generalization of the Adams–Bashford–Moulton algorithm. This method is based on a predictor–corrector scheme using the Caputo definition [53, 54]. In the following, the brief introduction of this algorithm and its generalization for a four-dimensional fractional-order system is given.

Consider the following differential equation:

$$D_t^\alpha y(t) = \frac{d^\alpha y(t)}{dt^\alpha} = f(t, y(t)), \quad 0 \leq t \leq T, \quad (11)$$

$$y^{(k)}(0) = y_0^{(k)}, \quad k = 0, 1, \dots, m - 1 (m = \lceil \alpha \rceil)$$

which is equivalent to the Volterra integral equation [55]

$$y(t) = \sum_{k=0}^{m-1} y_0^{(k)} \frac{t^k}{k!} + \frac{1}{\Gamma(\alpha)} \int_0^t \frac{f(s, y(s))}{(t-s)^{1-\alpha}} ds, \quad (12)$$

where  $\Gamma(\cdot)$  is the Gamma function, which is defined as

$$\Gamma(\alpha) = \int_0^\infty e^{-t} t^{\alpha-1} dt. \quad (13)$$

Set  $h = T/N, t_n = nh (n = 0, 1, 2, \dots, N)$ . Then (12) can be discretized as

$$y_h(t_{n+1}) = \sum_{k=0}^{m-1} y_0^{(k)} \frac{t_{n+1}^k}{k!} + \frac{h^\alpha}{\Gamma(\alpha + 2)} f(t_{n+1}, y_h^p(t_{n+1})) + \frac{h^\alpha}{\Gamma(\alpha + 2)} \sum_{j=0}^n a_{j,n+1} f(t_j, y_h(t_j)), \quad (14)$$

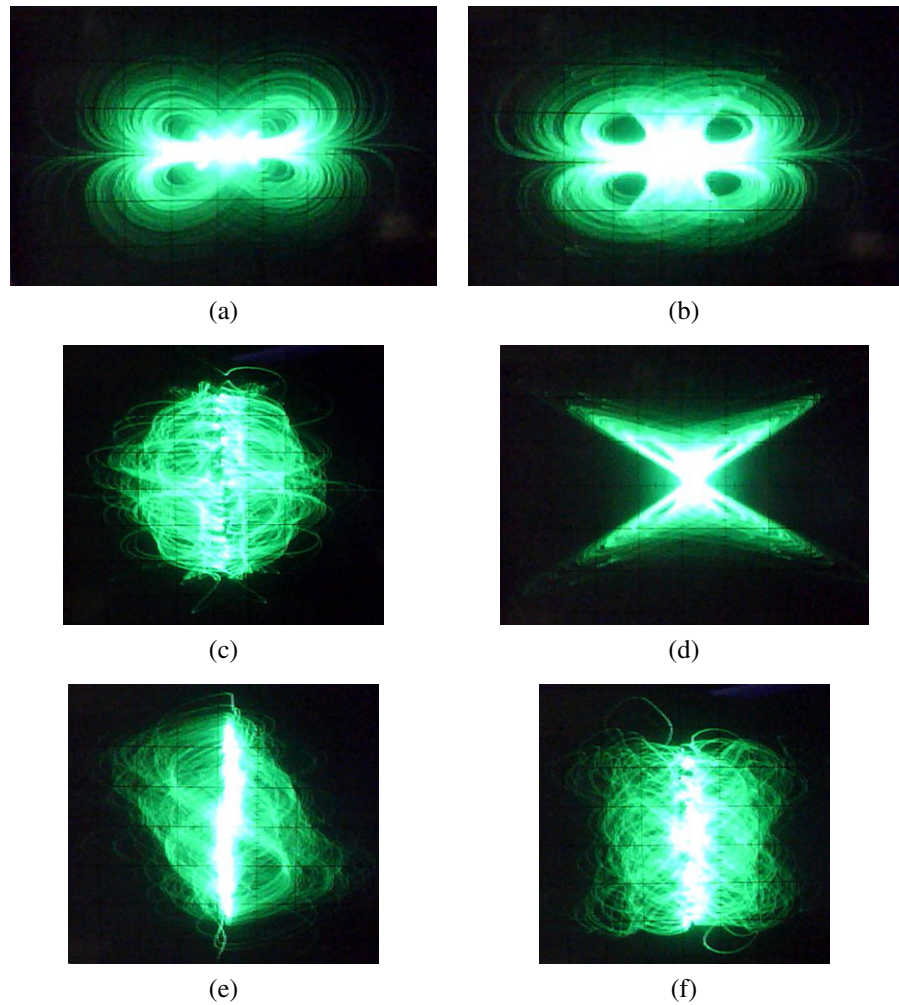
where a predicted value  $y_h^p(t_{n+1})$  is determined by

$$y_h^p(t_{n+1}) = \sum_{k=0}^{m-1} y_0^{(k)} \frac{t_{n+1}^k}{k!} + \frac{1}{\Gamma(\alpha)} \sum_{j=0}^n b_{j,n+1} f(t_j, y_h(t_j)) \quad (15)$$

in which



**Fig. 8** Phase portraits of the four-wing hyperchaotic attractor for  $a = 8, b = 40, c = 14.9$  observed on the oscilloscope: **(a)** projection on  $x-y$  plane, **(b)** projection on  $x-z$  plane, **(c)** projection on  $x-w$  plane, **(d)** projection on  $y-z$  plane, **(e)** projection on  $y-w$  plane, **(f)** projection on  $z-w$  plane



$$a_{j,n+1} = \begin{cases} n^{\alpha+1} - (n - \alpha)(n + 1)^\alpha, & j = 0 \\ (n - j + 2)^{\alpha+1} + (n - j)^{\alpha+1} - 2(n - j + 1)^{\alpha+1}, & 1 \leq j \leq n \\ 1, & j = n + 1, \end{cases}$$

$$b_{j,n+1} = \frac{h^\alpha}{\alpha} ((n - j + 1)^\alpha - (n - j)^\alpha).$$

(16)

The estimation error in this method is

$$e = \max |y(t_j) - y_h(t_j)| = O(h^p),$$

(17)

$(j = 0, 1, \dots, N)$

in which  $p = \min(2, 1 + \alpha)$ . Applying this method, numerical solution of a fractional-order system can be determined.

Now, consider the following fractional-order system:

$$\begin{cases} \frac{d^{\alpha_1} x}{dt^{\alpha_1}} = f_1(x, y, z, w) \\ \frac{d^{\alpha_2} y}{dt^{\alpha_2}} = f_2(x, y, z, w) \\ \frac{d^{\alpha_3} z}{dt^{\alpha_3}} = f_3(x, y, z, w) \\ \frac{d^{\alpha_4} w}{dt^{\alpha_4}} = f_4(x, y, z, w) \end{cases}$$

(18)

for  $0 < \alpha_i \leq 1 (i = 1, 2, 3, 4)$  and initial condition  $(x_0, y_0, z_0, w_0)$ . Applying the above method (Adams–Bashford–Moulton algorithm), system (18) can be discretized as follows:

$$\begin{cases} x_{n+1} = x_0 + \frac{h^{\alpha_1}}{\Gamma(\alpha_1+2)} [f_1(x_{n+1}^p, y_{n+1}^p, z_{n+1}^p, w_{n+1}^p) + \sum_{j=0}^n \gamma_{1,j,n+1} f_1(x_j, y_j, z_j, w_j)] \\ y_{n+1} = y_0 + \frac{h^{\alpha_2}}{\Gamma(\alpha_2+2)} [f_2(x_{n+1}^p, y_{n+1}^p, z_{n+1}^p, w_{n+1}^p) + \sum_{j=0}^n \gamma_{2,j,n+1} f_2(x_j, y_j, z_j, w_j)] \\ z_{n+1} = z_0 + \frac{h^{\alpha_3}}{\Gamma(\alpha_3+2)} [f_3(x_{n+1}^p, y_{n+1}^p, z_{n+1}^p, w_{n+1}^p) + \sum_{j=0}^n \gamma_{3,j,n+1} f_3(x_j, y_j, z_j, w_j)] \\ w_{n+1} = w_0 + \frac{h^{\alpha_4}}{\Gamma(\alpha_4+2)} [f_4(x_{n+1}^p, y_{n+1}^p, z_{n+1}^p, w_{n+1}^p) + \sum_{j=0}^n \gamma_{4,j,n+1} f_4(x_j, y_j, z_j, w_j)], \end{cases} \tag{19}$$

where

$$\begin{aligned} x_{n+1}^p &= x_0 + \frac{1}{\Gamma(\alpha_1)} \sum_{j=0}^n \xi_{1,j,n+1} f_1(x_j, y_j, z_j, w_j) \\ y_{n+1}^p &= y_0 + \frac{1}{\Gamma(\alpha_2)} \sum_{j=0}^n \xi_{2,j,n+1} f_2(x_j, y_j, z_j, w_j) \\ z_{n+1}^p &= z_0 + \frac{1}{\Gamma(\alpha_3)} \sum_{j=0}^n \xi_{3,j,n+1} f_3(x_j, y_j, z_j, w_j) \\ w_{n+1}^p &= w_0 + \frac{1}{\Gamma(\alpha_4)} \sum_{j=0}^n \xi_{4,j,n+1} f_4(x_j, y_j, z_j, w_j) \end{aligned} \tag{20}$$

and

$$\gamma_{i,j,n+1} = \begin{cases} n^{\alpha_i+1} - (n - \alpha_i)(n + 1)^{\alpha_i}, & j = 0 \\ (n - j + 2)^{\alpha_i+1} + (n - j)^{\alpha_i+1} - 2(n - j + 1)^{\alpha_i+1}, & 1 \leq j \leq n \\ 1, & j = n + 1, \end{cases} \tag{21}$$

$$\xi_{i,j,n+1} = \frac{h^{\alpha_i}}{\alpha_i} ((n - j + 1)^{\alpha_i} - (n - j)^{\alpha_i}).$$

The other method for numerical simulation of the fractional-order systems is the frequency-domain method which is based on the Bode diagram [56]. Utilizing this method, a higher-order linear model is obtained as an approximation for the fractional-order system. The order of this linear approximation system depends on the desired bandwidth and accuracy. However, in [57] it is declared that the first method (time-domain method) results are more reliable for simulating the fractional-order systems than the frequency-based method. So, in the simulations of this paper, we use the predictor–corrector scheme based method to solve the fractional-order differential equations.

### 8 Fractional-order form of the new chaotic system

In this section, we consider the fractional-order form of the new system, where integer-order derivatives are replaced by fractional-order ones. Mathematical description of the fractional-order chaotic system is expressed as

$$\begin{cases} D^{q_1} x = ax - yz + w, \\ D^{q_2} y = xz - by, \\ D^{q_3} z = xy - cz + xw, \\ D^{q_4} w = -y, \end{cases} \tag{22}$$

where  $q_1, q_2, q_3$  and  $q_4$  are the derivative orders.

For numerical simulation of fractional-order system (22), we have considered two cases: first, commensurate order system and second, non-commensurate order system. In the first case, it is assumed that the orders of the derivatives in state equations (22) are the same, i.e.  $q_1 = q_2 = q_3 = q_4 = q$ . Figure 9 shows the four-wing chaotic attractor generated from system (22) with the system parameters  $a = 8, b = 40$  and  $c = 14.9$ , and the commensurate order  $q = 0.95$  of the derivatives. When assuming the different orders of derivatives in state equations (22), i.e.  $q_1 \neq q_2 \neq q_3 \neq q_4$ , it gets a general non-commensurate order system. There is no exact condition for determining the orders to obtain chaotic behavior of the system. Figure 10 illustrates that the system is chaotic with  $q_1 = 1, q_2 = 0.95, q_3 = 0.9, q_4 = 0.85$ . It can be seen that the non-commensurate fractional-order system (22) can also generate a four-wing attractor.

### 9 Conclusion

In this letter, a new four-dimensional smooth system with a rare phenomenon was introduced and confirmed analytically and numerically. This new system has only one equilibrium point for any arbitrary set of parameters. Nevertheless, the most important fact

**Fig. 9** Phase portraits of the commensurate fractional-order four-wing chaotic attractor for  $a = 8, b = 40, c = 14.9$

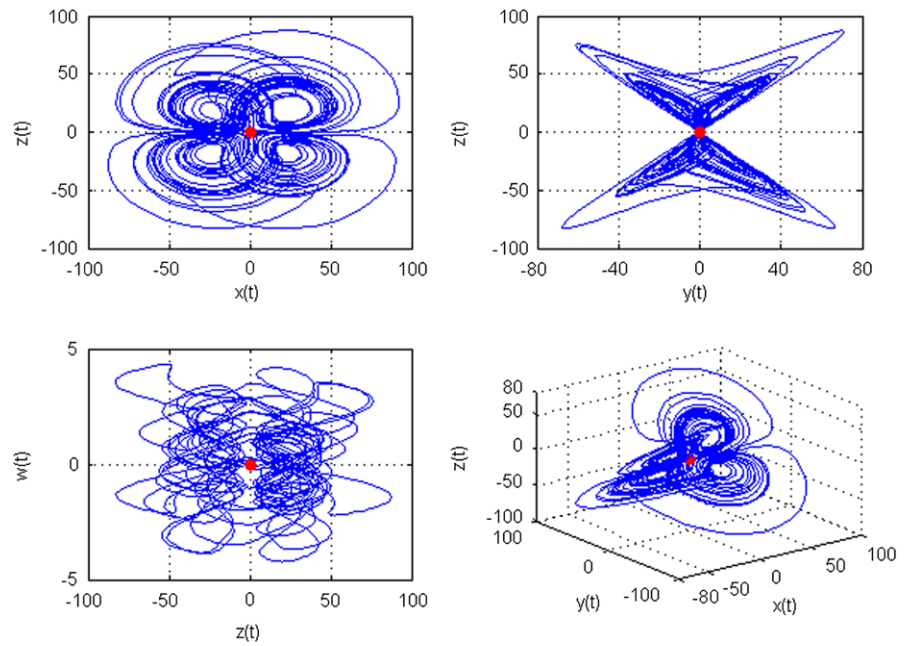
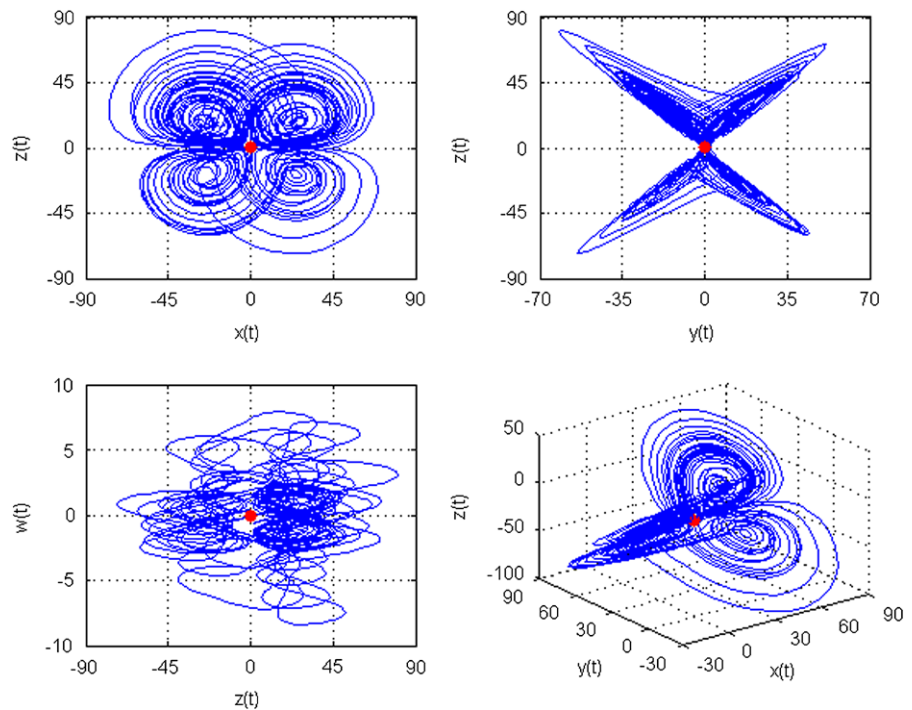


**Fig. 10** Phase portraits of the non-commensurate fractional-order four-wing chaotic attractor for  $a = 8, b = 40, c = 14.9$



about this system is that it can display four-wing hyperchaotic and chaotic attractors. Some dynamic behaviors of the system have been investigated. Furthermore, by electronic circuit implementation of the proposed system, it is shown that the four-wing hyper-

chaotic attractor does physically exist. Another interesting finding about this system is that it can generate a chaotic four-wing attractor when the total order is less than 4. This new system needs to be further studied and explored in both integer-order and fractional-order

cases, and its topological structure deserves further detailed investigation.

**Acknowledgements** Authors would like to thank the anonymous referees and Dr. J. Haseli for their valuable comments and suggestions.

## References

- Lorenz, E.N.: Deterministic nonperiodic flow. *J. Atmos. Sci.* **20**, 130–141 (1963)
- Chakravorty, J., Banerjee, T., Ghatak, R., Bose, A., Sarkar, B.C.: Generating chaos in injection-synchronized Gunn oscillator: an experimental approach. *IETE J. Res.* **55**, 106–111 (2009)
- Nana, B., Wofo, P., Domngang, S.: Chaotic synchronization with experimental application to secure communication. *Commun. Nonlinear Sci. Numer. Simul.* **14**, 629–655 (2009)
- Coulon, M., Roviras, D.: Multi-user receivers for synchronous and asynchronous transmission for chaos-based multiple-access systems. *Signal Process.* **89**, 583–598 (2009)
- Kozic, S., Hasler, M.: Low-density codes based on chaotic systems for simple encoding. *IEEE Trans. Circuits Syst. I* **56**, 405–415 (2009)
- Chen, G., Ueta, T.: Yet another chaotic attractor. *Int. J. Bifurc. Chaos* **9**, 1465–1466 (1999)
- Lü, J., Chen, G.: A new chaotic attractor coined. *Int. J. Bifurc. Chaos* **12**, 659–661 (2002)
- Qi, G., Chen, G., Du, S., Chen, Z., Yuan, Z.: Analysis of a new chaotic system. *Physica A* **352**, 295–308 (2005)
- Wang, G.Y., Qui, S.S., Li, H.W., Li, C.F., Zheng, Y.: A new chaotic system and its circuit realization. *Chin. Phys. B* **15**, 2872–2877 (2006)
- Liu, C., Liu, L.: A new three-dimensional autonomous chaotic oscillation system. *J. Phys. Conf. Ser.* **96**, 012173 (2008)
- Chen, Z., Yang, Y., Yuan, Z.: A single three-wing or four-wing chaotic attractor generated from a three-dimensional smooth quadratic autonomous system. *Chaos Solitons Fractals* **38**, 1187–1196 (2008)
- Wang, L.: 3-scroll and 4-scroll chaotic attractors generated from a new 3-D quadratic autonomous system. *Nonlinear Dyn.* **56**, 453–462 (2009)
- Dadras, S., Momeni, H.R.: A novel three-dimensional autonomous chaotic system generating two-, three- and four-scroll attractors. *Phys. Lett. A* **373**, 3637–3642 (2009)
- Baghious, E., Jarry, P.: Lorenz attractor: From differential equations with piecewise-linear terms. *Int. J. Bifurc. Chaos* **3**, 201–210 (1993)
- Elwakil, A., Ozoguz, S., Kennedy, M.: Creation of a complex butterfly attractor using a novel Lorenz-type system. *IEEE Trans. Circuits Syst. I* **49**, 527–530 (2002)
- Ozoguz, S., Elwakil, A., Kennedy, M.: Experimental verification of the butterfly attractor in a modified Lorenz system. *Int. J. Bifurc. Chaos* **12**, 1627–1632 (2002)
- Qi, G., Chen, G., Li, S., Zhang, Y.: Four-wing attractors: From pseudo to real. *Int. J. Bifurc. Chaos* **16**, 859–885 (2006)
- Grassi, G., Severance, F.L., Mashev, E.D., Bazuin, B.J., Miller, D.A.: Generation of a four-wing chaotic attractor by two weakly-coupled Lorenz systems. *Int. J. Bifurc. Chaos* **18**, 2089–2094 (2008)
- Grassi, G.: Novel four-wing and eight-wing attractors using coupled chaotic Lorenz systems. *Chin. Phys. B* **17**, 3247–3251 (2008)
- Dadras, S., Momeni, H.R., Qi, G.: Analysis of a new 3D smooth autonomous system with different wing chaotic attractors and transient chaos. *Nonlinear Dyn.* **62**, 391–405 (2010)
- Wang, L.: Yet another 3D quadratic autonomous system generating three-wing and four-wing chaotic attractors. *Chaos* **19**, 013107 (2009)
- Dadras, S., Momeni, H.R.: Generating one-, two-, three- and four-scroll attractors from a novel four-dimensional smooth autonomous chaotic system. *Chin. Phys. B* **19**, 060506 (2010)
- Rössler, O.E.: An equation for hyperchaos. *Phys. Lett. A* **71**, 155–157 (1979)
- Thamilmaran, K., Lakshmanan, M., Venkatesan, A.: Hyperchaos in a modified canonical Chua's circuit. *Int. J. Bifurc. Chaos* **14**, 221–243 (2004)
- Li, Y., Tang, S.K., Chen, G.: Generating hyperchaos via state feedback control. *Int. J. Bifurc. Chaos* **15**, 3367–3375 (2005)
- Li, Y., Tang, W.K.S., Chen, G.: Hyperchaos evolved from the generalized Lorenz equation. *Int. J. Circuit Theory Appl.* **33**, 235–251 (2005)
- Wang, J.Z., Chen, Z.Q., Yuan, Z.Z.: The generation of a hyperchaotic system based on a three-dimensional autonomous chaotic system. *Chin. Phys. B* **15**, 1216–1225 (2006)
- Jia, Q.: Generation and suppression of a new hyperchaotic system with double hyperchaotic attractors. *Phys. Lett. A* **371**, 410–415 (2007)
- Jia, Q.: Hyperchaos generated from the Lorenz chaotic system and its control. *Phys. Lett. A* **366**, 217–222 (2007)
- Qi, G., Wyk, M.A., Wyk, B.J., Chen, G.: On a new hyperchaotic system. *Phys. Lett. A* **372**, 124–136 (2008)
- Liu, L., Liu, C., Zhang, Y.: Analysis of a novel four-dimensional hyperchaotic system. *Chin. J. Phys.* **46**, 386–393 (2008)
- Wu, W.J., Chan, Z.Q., Yuan, Z.Z.: Local bifurcation analysis of a four-dimensional hyperchaotic system. *Chin. Phys. B* **17**, 2420–2432 (2008)
- Mahmoud, G.M., Al-Kashif, M.A., Farghaly, A.A.: Chaotic and hyperchaotic attractors of a complex nonlinear system. *J. Phys. A, Math. Theor.* **41**, 055104 (2008)
- Yujun, N., Xingyuan, W., Mingjun, W., Huaguang, Z.: A new hyperchaotic system and its circuit implementation. *Commun. Nonlinear Sci. Numer. Simul.* **15**, 3518–3524 (2010)
- Zheng, S., Dong, G., Bi, Q.: A new hyperchaotic system and its synchronization. *Appl. Math. Comput.* **215**, 3192–3200 (2010)
- Mahmoud, G.M., Mahmoud, E.E., Ahmed, M.E.: On the hyperchaotic complex Lü system. *Nonlinear Dyn.* **58**, 725–738 (2009)
- Qi, G., Wyk, M.A., Wyk, B.J., Chen, G.: A new hyperchaotic system and its circuit implementation. *Chaos Solitons Fractals* **40**, 2544–2549 (2009)

38. Yang, Q., Zhang, K., Chen, G.: Hyperchaotic attractors from a linearly controlled Lorenz system. *Nonlinear Anal., Real World Appl.* **10**, 1601–1617 (2009)
39. Chen, C.H., Sheu, L.J., Chen, H.K., Chen, J.H., Wang, H.C., Chao, Y.C., Lin, Y.K.: A new hyper-chaotic system and its synchronization. *Nonlinear Anal., Real World Appl.* **10**, 2088–2096 (2009)
40. Chen, Z., Yang, Y., Qi, G., Yuan, Z.: A novel hyperchaos system only with one equilibrium. *Phys. Lett. A* **360**, 696–701 (2007)
41. Liu, C.: A new hyperchaotic dynamical system. *Chin. Phys.* **16**, 3279–3284 (2007)
42. Cang, S., Qi, G., Chen, Z.: A four-wing hyper-chaotic attractor and transient chaos generated from a new 4-D quadratic autonomous system. *Nonlinear Dyn.* **59**, 515–527 (2010)
43. Grassi, G., Severance, F.L., Miller, D.A.: Multi-wing hyperchaotic attractors from coupled Lorenz systems. *Chaos Solitons Fractals* **41**, 284–291 (2009)
44. Makris, N., Constantinou, M.C.: Fractional derivative Maxwell model for viscous dampers. *J. Struct. Eng.* **117**, 2708–2724 (1991)
45. Scalas, E., Gorenflo, R., Mainardi, F.: Fractional calculus and continuous-time finance. *Physica A* **284**, 376–384 (2000)
46. Cafagna, D.: Fractional calculus: a mathematical tool from the past for present engineers. *IEEE Ind. Electron. Mag.* (summer), 35–40 (2007)
47. Tavazoei, M.S., Haeri, M., Bolouki, S., Siami, M.: Using fractional-order integrator to control chaos in single-input chaotic system. *Nonlinear Dyn.* **55**, 179–190 (2009)
48. Cafagna, D., Grassi, G.: Bifurcation and chaos in the fractional-order Chen system via a time-domain approach. *Int. J. Bifurc. Chaos* **18**, 1845–1863 (2008)
49. Cafagna, D., Grassi, G.: Fractional-order Chua's circuit: time domain analysis, bifurcation, chaotic behavior and test for chaos. *Int. J. Bifurc. Chaos* **18**, 615–639 (2008)
50. Daftardar-Gejji, V., Bhalekar, S.: Chaos in fractional ordered Liu system. *Comput. Math. Appl.* **59**, 1117–1127 (2010)
51. Cafagna, D., Grassi, G.: Fractional-order chaos: a novel four-wing attractor in coupled Lorenz systems. *Int. J. Bifurc. Chaos* **19**, 3329–3338 (2009)
52. Cafagna, D., Grassi, G.: Hyperchaos in the fractional-order Rössler system with lowest order. *Int. J. Bifurc. Chaos* **19**, 339–347 (2009)
53. Diethelm, K.: An algorithm for the numerical solution of differential equations of fractional order. *Electron. Trans. Numer. Anal.* **5**, 1–6 (1997)
54. Diethelm, K., Ford, N.J., Freed, A.D.: A predictor-corrector approach for the numerical solution for fractional differential equations. *Nonlinear Dyn.* **29**, 3–22 (2002)
55. Diethelm, K., Ford, N.J.: Analysis of fractional differential equations. *J. Math. Anal. Appl.* **265**, 229–248 (2002)
56. Charef, A., Sun, H.H., Tsao, Y.Y., Onaral, B.: Fractal systems as represented by singularity function. *IEEE Trans. Autom. Control* **37**, 1465–1470 (1992)
57. Tavazoei, M.S., Haeri, M.: Limitation of frequency domain approximation for detecting chaos in fractional-order system. *Nonlinear Anal. Theory Methods Appl.* **69**, 1299–1320 (2008)